research communications

Crystal structure of bis(*N*,*N*′-dimethylthiourea-*κS*)-bis(thiocyanato-*κN*)cobalt(II)

Aleksej Jochim,* Rastko Radulovic, Inke Jess and Christian Näther

Institut für Anorganische Chemie, Christian-Albrechts-Universität Kiel, Max-Eyth-Str. 2, D-24118 Kiel, Germany. *Correspondence e-mail: ajochim@ac.uni-kiel.de

During systematic investigations on the synthesis of coordination polymers with $Co(NCS)_2$ involving different thiourea derivatives as coligands, crystals of the title compound $Co(NCS)_2(N,N'$-dimethylthiourea$)_2$, or $[Co(C_3H_8N_2S)_2(NCS)_2]$, were obtained. These crystals were non-merohedral twins and therefore, a twin refinement using data in HKLF-5 format was performed. In the crystal structure of this compound, the Co^{II} cations are coordinated by two N-terminally bonded thiocyanate anions as well as two S-bonding *N*,*N*′-dimethylthiourea molecules, forming two crystallographically independent discrete complexes each with a strongly distorted tetrahedral geometry. An intricate network of intermolecular N—H⋯S and C—H⋯S hydrogen bonds can be found between the complexes. The thermogravimetric curve of the title compound shows two discrete steps in which all coligand molecules have been emitted, which is also accompanied by partial decomposition of the cobalt thiocyanate. If the measurement is stopped after the first mass loss, only broad reflections of CoS can be found in the XRPD pattern of the residue, which proves that this compound decomposes completely upon heating. However, at lower temperatures an endothermic signal can be found in the DTA and DSC curve, which corresponds to melting, as proven by thermomicroscopy.

1. Chemical context

Investigations on the synthesis, crystal structures and magnetic properties of coordination polymers based on transition-metal thiocyanates have become of increasing interest in recent years, which is due to the high structural diversity of the thiocyanate anion and its ability to mediate reasonable magnetic exchange. Although many different transition-metal thiocyanate coordination compounds are known, our main interests focus on first-row transition-metal thiocyanate compounds with the general composition $M(NCS)_2(L)_2$ in which paramagnetic metal cations *M* are connected by pairs of *μ*-1,3 bridging thiocyanate anions into chains, while the remaining coordination sites are occupied by neutral coligands *L*, forming an octahedral coordination polyhedron. In most of these compounds, linear chains are formed in which all ligands are *trans* (Prananto *et al.*, 2017; Werner *et al.*, 2015a; Mautner *et al.*, 2018; Rams *et al.*, 2020; Jin *et al.*, 2007), but other isomers are also possible. This includes compounds in which either the N-bonding thiocyanates, the S-bonding thiocyanates or the coligands are *trans*, while the other ligands are *cis*. These motifs are found, for example, in $[M(NCS)_2(4$-benzyl-pyridine$)_2]_n$ (*M* = Mn, Ni, Cd) (Suckert *et al.*, 2015; Jochim *et al.*, 2018; Neumann *et al.*, 2018a), $[M(NCS)_2(4$-nitropyridine *N*-oxide$)_2]_n$ (*M* = Mn, Co, Cd) (Shi *et al.*, 2006, 2007; Mautner *et al.*, 2016) and $[M(NCS)_2(4$-benzoylpyridine$)_2]_n$ (*M* = Co, Ni)

Co
N
C
S
H
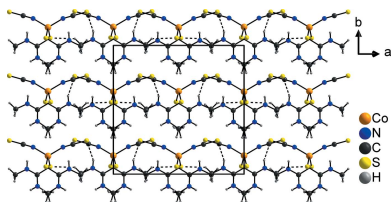
(Rams *et al.*, 2017; Jochim *et al.*, 2018), in which different *cis–cis–trans* configurations can be found around the metal centers. The last possible isomer, in which all ligands are *cis*, is not found for the composition $M(NCS)_2(L)_2$, although it was observed in more ligand-deficient compounds of composition $Co(NCS)_2(L)$, with *L* representing either 4-methylpyridine *N*-oxide or 4-methoxypyridine *N*-oxide (Zhang *et al.*, 2006*a*,*b*).

In those cases in which either only the N-bonding or the S-bonding thiocyanate are *cis*, corrugated chains are formed instead of linear ones, which is also the case if all ligands are *cis*. Furthermore, in some compounds a mixture of these configurations can be found, as in $[M(NCS)_2(4\text{-chloro-pyridine})_2]_n$ (*M* = Co, Ni, Cd) (Böhme *et al.*, 2020; Jochim *et al.*, 2018; Goher *et al.*, 2003) or the high-temperature modification of $[Ni(NCS)_2(4\text{-aminopyridine})_2]_n$ (Neumann *et al.*, 2018*b*), in which an alternating arrangement of all-*trans* and *cis–cis–trans*-coordinated metal cations is present.

For some compounds of composition $M(NCS)_2(L)_2$ a completely different structure is observed, in which the metal cations are connected into layers of different topologies by the thiocyanate anions. Only one topology is known for cobalt compounds of this composition, in which every two cobalt cations are connected by a pair of μ-1,3-bridging thiocyanate anions, forming dimers, which are connected to four adjacent dimers by single μ-1,3-bridging thiocyanate anions (Wöhlert & Näther, 2013; Suckert *et al.*, 2016, 2017; Werner *et al.*, 2015*b*). Nevertheless, with other metal cations different layer topologies are known in which, for example, trimers are formed instead of dimers, which are connected by single μ-1,3-thiocyanate bridges (Kozísková *et al.*, 1990; Kabešová *et al.*, 1990) or in which each metal cation is directly connected to four neighboring metal cations by single μ-1,3-thiocyanate bridges (McElearney *et al.*, 1979; Werner *et al.*, 2015*c*; Đaković *et al.*, 2010). Although it is not clear by which parameters the formation of either chains or layers is promoted, a third isomer of composition $Co(NCS)_2(L)_2$ exists in which the thiocyanate anions are N-terminally coordinated, forming discrete tetrahedral complexes (Prananto *et al.*, 2017; Neumann *et al.*, 2018*c*; Hannachi *et al.*, 2019). In most of these compounds, electron-rich coligands are found, which might indicate that this type of compound is formed when a strong donor is used as coligand.

Most of the aforementioned compounds contain N-donor coligands, but in the course of our systematic work we became interested in the influence of S-donor coligands based on thiourea derivatives on the magnetic properties of $Co(NCS)_2$ chain compounds, in which the metal cations are linked by pairs of μ-1,3-bridging thiocyanate anions. With nickel, two compounds with the composition $Ni(NCS)_2(\text{ethylenethiourea})_2$ (Nardelli *et al.*, 1966) and $Ni(NCS)_2(\text{thioacetamide})_2$ (Capacchi *et al.*, 1968) are known. We prepared the corresponding cobalt compound with ethylenethiourea, which is isotypic to the nickel analogue (Jochim *et al.*, 2020*a*). Only one additional polymeric compound with the composition $[Co(NCS)_2(\text{thiourea})_2]_n$ is known, in which the cobalt cations are connected by the sulfur atoms of the coligands, while the thiocyanate anions are N-terminally coordinated (Rajarajan *et al.*, 2012; Muthu *et al.*, 2015). In further work we prepared $Co(NCS)_2(\text{tetramethylthiourea})_2$, which surprisingly consists of discrete tetrahedral complexes (Jochim *et al.*, 2020*b*).
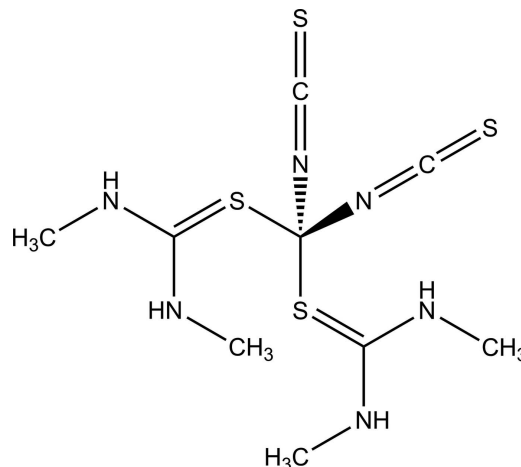
To further investigate this structural behavior, we used N,N'-dimethylthiourea as coligand, which is between thiourea and tetramethylthiourea considering the substitution with methyl groups, and during these investigations the title compound was obtained. Its IR spectrum shows that the C—N stretching vibration is found at 2064 cm^{-1}, which is indicative of N-terminally bonded thiocyanate anions, pointing to the formation of a tetrahedral complex, as proven by single crystal X-ray diffraction (see Fig. S1 in the supporting information). Although the experimental XRPD pattern is very similar to that calculated for the title compound, some additional reflections are found, indicating some contamination (Fig. S2). This is surprising, because all samples were prepared in different ways and using a different ratio of $Co(NCS)_2$ and dimethylthiourea leads to an identical XRPD pattern. In the thermogravimetry curve (Fig. S3), two mass losses of 37.2% and 26.3% are observed, which in total is more than expected for the emission of both coligand molecules (54.3%), indicating the decomposition of the thiocyanate anions. This was proven by PXRD of the residue isolated after the first mass loss, which is mostly amorphous but which contains a small amount of crystalline CoS (Fig. S4). At low temperatures, an additional endothermic event can be found in the differential thermoanalysis curve, which is not accompanied by a mass change of the sample. This event corresponds to melting of the sample and is not reversible upon cooling, which was shown by differential scanning calorimetry (Fig. S5) and thermomicroscopy (Fig. S6).

2. Structural commentary

The asymmetric unit of the title compound contains two crystallographically independent complexes built up of two thiocyanate anions and two N,N'-dimethylthiourea molecules in general positions as well as one cobalt(II) cation, which is situated on a twofold rotational axis in both crystallographically independent complexes. Both metal cations are coordinated by two N-bonding thiocyanate anions and two
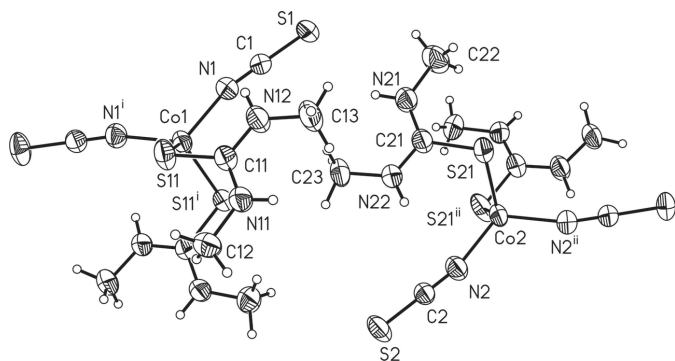
Figure 1
View of the two crystallographically independent molecules in the asymmetric unit of the title compound with atom labeling and displacement ellipsoids drawn at the 50% probability level. Symmetry codes: (i) $-x + 1, y, -z + \frac{3}{2}$; (ii) $-x, y, -z + \frac{1}{2}$.

S-bonding N,N'-dimethylthiourea molecules, forming strongly distorted tetrahedra (Fig. 1), which becomes obvious from the tetrahedral angle variance $\sigma_{\theta\langle\text{tet}\rangle}^2 = 73.2$ (Co1) or 73.3 (Co2) and the mean tetrahedral quadratic elongation $\langle\lambda_{\text{tet}}\rangle = 1.030$ (Co1, Co2) (Robinson *et al.*, 1971). However, all bond lengths and angles are comparable to those reported for similar compounds in the literature (Neumann *et al.* 2018c). Both N,N'-dimethylthiourea molecules are nearly planar with C_{Me}—N—C—N torsion angles of 177.7 (3) and -0.5 (4)° for the complex containing Co1 and 178.9 (3) and -1.2 (4)° for that containing Co2. Both N,N'-dimethylthiourea planes within each complex are slightly tilted relative to each other, leading to an angle of 9.51 (10)° between the normal vectors of the N,N'-dimethylthiourea planes in the complex containing Co1, while the corresponding angle for the complex containing Co2 is 13.52 (8)°. Similar values are observed for the corresponding angles between the N,N'-dimethylthiourea planes of different crystallographically independent complexes.

3. Supramolecular features

The discrete complexes are connected *via* relatively weak N—H···S_{NCS} hydrogen bonds (Table 1), forming chains along the [101] direction in which the two crystallographically independent discrete complexes alternate. For both complexes, either only the thiocyanate anions (Co1) or the N,N'-dimethylthiourea molecules (Co2) are involved in the formation of this structure. Two neighboring chains are connected into double chains by pairs of additional N—H···S_{NCS} hydrogen bonds involving only the complexes containing Co1 (Fig. 2). In a similar way, chains built up of an alternating sequence of complexes containing either Co1 or Co2 are formed, which run along the *a*-axis direction, but in this case, in the complexes containing Co1, only the N,N'-dimethylthiourea molecules participate in the N—H···S_{NCS} hydrogen bonds, while in the complex containing Co2, only the thiocyanate anions are involved. Within these chains, additional C—H···S hydrogen bonds between the N,N'-dimethylthiourea molecules of adjacent complexes can be found (Fig. 3). The two

Table 1
Hydrogen-bond geometry (Å, °).

D—H···A	D—H	H···A	D···A	D—H···A
N11—H11···S1[i]	0.88	2.65	3.341 (2)	136
N12—H12···N1	0.88	2.69	3.282 (3)	126
N12—H12···S2[ii]	0.88	2.88	3.582 (2)	138
C13—H13B···S21[iii]	0.98	2.80	3.578 (3)	137
N21—H21···S1	0.88	2.61	3.372 (2)	146
C22—H22A···S2[iv]	0.98	3.01	3.591 (3)	120
C22—H22A···S21[iii]	0.98	3.02	3.752 (4)	132
N22—H22···S2[v]	0.88	2.79	3.486 (3)	137

Symmetry codes: (i) $-x + \frac{1}{2}, y + \frac{1}{2}, -z + \frac{3}{2}$; (ii) $x, -y + 1, z + \frac{1}{2}$; (iii) $-x, -y + 1, -z + 1$; (iv) $x - \frac{1}{2}, y - \frac{1}{2}, z$; (v) $-x + \frac{1}{2}, -y + \frac{3}{2}, -z + 1$.

types of chain are connected *via* C—H···S hydrogen bonds between the N,N'-dimethylthiourea molecules, forming layers parallel to the *ac* plane (Fig. 4), which are further connected into a three-dimensional network by additional N—H···S_{NCS} hydrogen bonds.

4. Database survey

In the Cambridge Structure Database (Version 5.41, last update November 2019; Groom *et al.*, 2016), only one transition-metal thiocyanate compound with N,N'-dimethylthio-
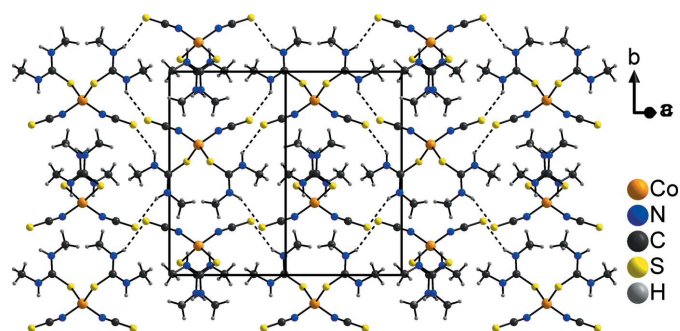
Figure 2
Crystal structure of the title compound with a view of the chains that extend along [101]. Intermolecular N—H···S hydrogen bonding is shown as dashed lines.
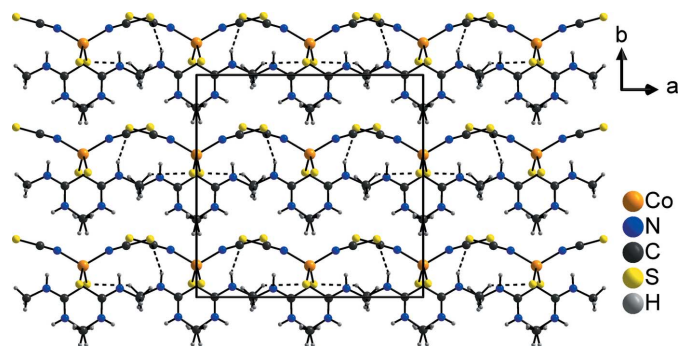
Figure 3
Crystal structure of the title compound with a view of the chains that extend along the *a*-axis direction. Intermolecular N—H···S and C—H···S hydrogen bonds are shown as dashed lines.
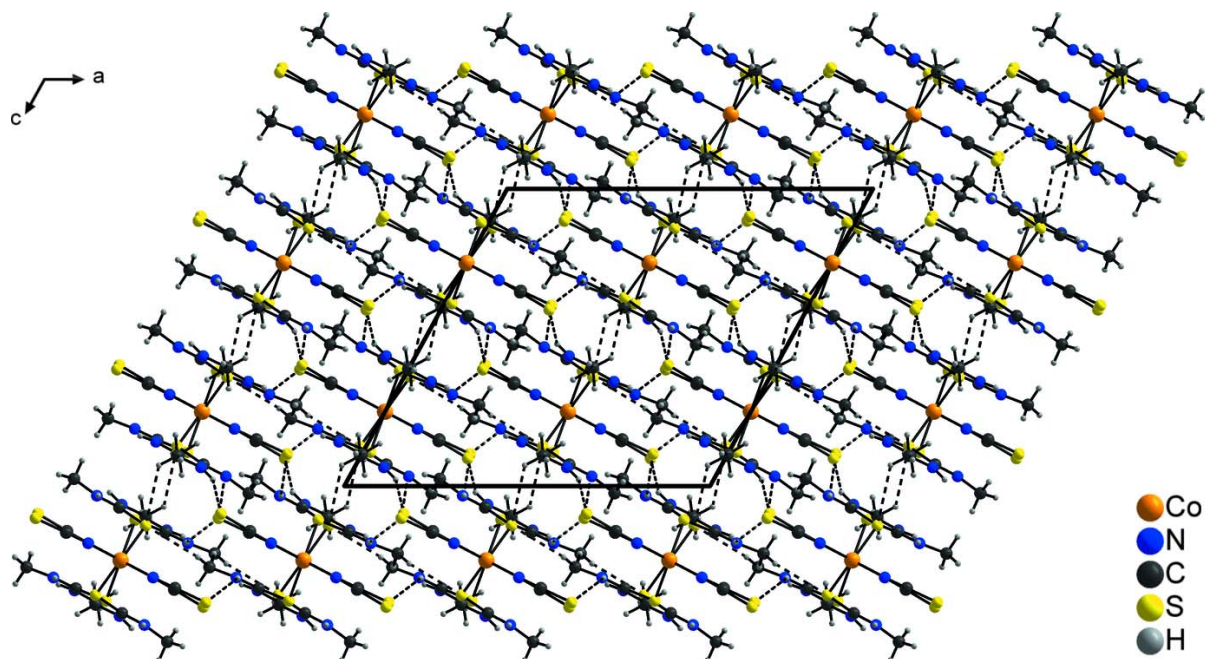
Figure 4
Crystal structure of the title compound with a view perpendicular to the layers parallel to the crystallographic *ac* plane. Intermolecular N—H···S and C—H···S hydrogen bonds are shown as dashed lines.

urea is reported, which has the composition Cu(NCS)(*N*,*N*′-dimethylthiourea)[propane-1,3-diylbis(diphenylphosphine)] (Wattanakanjana *et al.*, 2015). In this compound, the Cu^I cations are tetrahedrally coordinated by one thiocyanate anion, one *N*,*N*′-dimethylthiourea molecule and one propane-1,3-diylbis(diphenylphosphine) molecule, with both phosphines coordinating to the metal center. In total, only 49 compounds containing a transition-metal cation and *N*,*N*′-dimethylthiourea are known, none of which contains cobalt. In fact, 28 of these compounds involve more chalcophilic second or third row transition-metal cations, while nearly half of the remaining compounds contain copper.

Considering compounds that contain cobalt thiocyanate, over one thousand compounds are found, most of which show either an octahedral or a tetrahedral coordination geometry with the octahedral coordination geometry being the most common. Nevertheless, approximately 200 compounds with tetrahedral coordination geometry are known, making it the second most common coordination geometry for cobalt thiocyanate compounds.

5. Synthesis and crystallization

General

N,*N*′-dimethylthiourea was purchased from Sigma Aldrich, while Co(NCS)$_2$ was purchased from Alfa Aesar. All chemicals were used without further purification.

Synthesis

Single crystals were obtained by reacting Co(NCS)$_2$ (0.15 mmol, 26.3 mg) with *N*,*N*′-dimethylthiourea (0.3 mmol, 31.3 mg) in 0.4 mL of water. After approximately one week, deep-blue crystals were obtained, which were suitable for single crystal analysis. The same procedure was used to obtain powder samples using a higher amount of Co(NCS)$_2$ (1.00 mmol, 175.1 mg), *N*,*N*′-dimethylthiourea (2.0 mmol, 208.4 mg) and water (0.75 mL). The resulting crystals were ground into powder. In some cases, no crystallization of the mixture occurred, which was prevented by storing the reaction mixture at 281 K. Elemental analysis calculated for C$_8$H$_{16}$N$_6$CoS$_4$ (383.45 g/mol) C 25.06%, H 4.21%, N 21.92%, S 33.45%, found: C 24.79%, H 4.34%, N 21.75%, S 32.16%.

Experimental details

Elemental analysis was performed using a EURO EA elemental analyzer fabricated by EURO VECTOR Instruments.

The IR spectrum was measured using an ATI Mattson Genesis Series FTIR Spectrometer, control software: WINFIRST, from ATI Mattson.

The PXRD measurement was performed with Cu *K*α$_1$ radiation (λ = 1.540598 Å) using a Stoe Transmission Powder Diffraction System (STADI P) equipped with a MYTHEN 1K detector and a Johansson-type Ge(111) monochromator.

DTA–TG measurements were performed in a dynamic nitrogen atmosphere (100 sccm) in Al$_2$O$_3$ crucibles using a STA-PT 1600 thermobalance from Linseis. The instrument was calibrated using standard reference materials.

The DSC measurements were performed with a DSC 1 Star System with STARe Excellence Software from Mettler–Toledo AG. The instrument was calibrated using standard reference materials.

Thermomicroscopic measurements were performed using an FP82 hot stage from Mettler and a BX60 microscope from Olympus, using the analysis software package from Mettler.

research communications

Table 2
Experimental details.

Crystal data

Chemical formula	[Co(C₃H₈N₂S)₂(NCS)₂]

Chemical formula: $[Co(C_3H_8N_2S)_2(NCS)_2]$

M_r	383.44
Crystal system, space group	Monoclinic, $C2/c$
Temperature (K)	200
a, b, c (Å)	16.8070 (8), 14.4212 (6), 15.5669 (9)
β (°)	118.744 (4)
V (Å³)	3308.1 (3)
Z	8
Radiation type	Mo $K\alpha$
μ (mm⁻¹)	1.54
Crystal size (mm)	0.10 × 0.08 × 0.07

Data collection

Diffractometer	Stoe IPDS2
No. of measured, independent and observed [$I > 2\sigma(I)$] reflections	3218, 3218, 2767
$(\sin \theta/\lambda)_{max}$ (Å⁻¹)	0.618

Refinement

$R[F^2 > 2\sigma(F^2)]$, $wR(F^2)$, S	0.039, 0.105, 1.07
No. of reflections	3218
No. of parameters	178
H-atom treatment	H-atom parameters constrained
$\Delta\rho_{max}$, $\Delta\rho_{min}$ (e Å⁻³)	0.72, −0.40

Computer programs: *X-AREA* and *XP* (Stoe & Cie, 2002), *SHELXS97* (Sheldrick, 2008), *SHELXL2018/3* (Sheldrick, 2015), *DIAMOND* (Brandenburg & Putz, 1999) and *publCIF* (Westrip, 2010).

6. Refinement

Crystal data, data collection and structure refinement details are summarized in Table 2. All non-hydrogen atoms were refined anisotropically. The C—H H atoms were positioned with idealized geometry and refined isotropically with $U_{iso}(H) = 1.5U_{eq}(C)$, allowing them to rotate, but not to tip. The N—H H atoms were located in the difference map, their bond lengths were set to ideal values and finally they were refined using a riding model [$U_{iso}(H) = 1.2U_{eq}(N)$]. As the crystal studied was twinned by non-merohedry, a twin refinement using data in HKLF 5 format was performed. The corresponding files were generated by *PLATON* (Spek 2020).

References

Đaković, M., Jagličić, Z., Kozlevčar, B. & Popović, Z. (2010). *Polyhedron*, **29**, 1910–1917.
Goher, M. A. S., Mautner, F. A., Abu-Youssef, M. A. M., Hafez, A. K., Badr, A. M.-A. & Gspan, C. (2003). *Polyhedron*, **22**, 3137–3143.
Groom, C. R., Bruno, I. J., Lightfoot, M. P. & Ward, S. C. (2016). *Acta Cryst.* B**72**, 171–179.
Hannachi, A., Valkonen, A., Rzaigui, M. & Smirani, W. (2019). *Polyhedron*, **161**, 222–230.
Jin, Y., Che, Y. X. & Zheng, J. M. (2007). *J. Coord. Chem.* **60**, 2067–2074.
Jochim, A., Lohmiller, T., Rams, M., Böhme, M., Ceglarska, M., Schnegg, A., Plass, W. & Näther, C. (2020a). *Inorg. Chem.* **59**, 8971–8982.
Jochim, A., Radulovic, R., Jess, I. & Näther, C. (2020b). *Acta Cryst.* E**76**, 1373–1377.
Jochim, A., Rams, M., Neumann, T., Wellm, C., Reinsch, H., Wójtowicz, G. M. & Näther, C. (2018). *Eur. J. Inorg. Chem.* pp. 4779–4789.
Kabešová, M., Kožíšková, Z. & Dunaj-Jurčo, M. (1990). *Collect. Czech. Chem. Commun.* **55**, 1184–1192.
Kozísková, Z., Kozisek, J. & Kabesová, M. (1990). *Polyhedron*, **9**, 1029–1034.
Mautner, F. A., Berger, C., Fischer, R. C. & Massoud, S. S. (2016). *Polyhedron*, **111**, 86–93.
Mautner, F. A., Traber, M., Fischer, R. C., Torvisco, A., Reichmann, K., Speed, S., Vicente, R. & Massoud, S. S. (2018). *Polyhedron*, **154**, 436–442.
McElearney, J. N., Balagot, L. L., Muir, J. A. & Spence, R. D. (1979). *Phys. Rev. B*, **19**, 306–317.
Muthu, K., Meenatchi, V., Rajasekar, M., Kanagarajan, V., Madhurambal, G., Meenakshisundaram, S. P. & Mojumdar, S. C. (2015). *J. Therm. Anal. Calorim.* **119**, 945–952.
Nardelli, M., Gasparri, G. F., Musatti, A. & Manfredotti, A. (1966). *Acta Cryst.* **21**, 910–919.
Neumann, T., Ceglarska, M., Germann, L. S., Rams, M., Dinnebier, R. E., Suckert, S., Jess, I. & Näther, C. (2018b). *Inorg. Chem.* **57**, 3305–3314.
Neumann, T., Jess, I., dos Santos Cunha, C., Terraschke, H. & Näther, C. (2018a). *Inorg. Chim. Acta*, **478**, 15–24.
Neumann, T., Jess, I., Pielnhofer, F. & Näther, C. (2018c). *Eur. J. Inorg. Chem.* pp. 4972–4981.
Prananto, Y. P., Urbatsch, A., Moubaraki, B., Murray, K. S., Turner, D. R., Deacon, G. B. & Batten, S. R. (2017). *Aust. J. Chem.* **70**, 516–528.
Rajarajan, K., Sendil Kumar, K., Ramesh, V., Shihabuddeen, V. & Murugavel, S. (2012). *Acta Cryst.* E**68**, m1125–m1126.
Rams, M., Jochim, A., Böhme, M., Lohmiller, T., Ceglarska, M., Rams, M. M., Schnegg, A., Plass, W. & Näther, C. (2020). *Chem. Eur. J.* **26**, 2837–2851.
Rams, M., Tomkowicz, Z., Böhme, M., Plass, W., Suckert, S., Werner, J., Jess, I. & Näther, C. (2017). *Phys. Chem. Chem. Phys.* **19**, 3232–3243.
Robinson, K., Gibbs, G. V. & Ribbe, P. H. (1971). *Science*, **172**, 567–570.
Sheldrick, G. M. (2008). *Acta Cryst.* A**64**, 112–122.
Sheldrick, G. M. (2015). *Acta Cryst.* C**71**, 3–8.
Shi, J.-M., Chen, J.-N. & Liu, L.-D. (2006). *Pol. J. Chem.* **80**, 1909–1913.
Shi, J.-M., Chen, J.-N., Wu, C.-J. & Ma, J.-P. (2007). *J. Coord. Chem.* **60**, 2009–2013.
Spek, A. L. (2020). *Acta Cryst.* E**76**, 1–11.
Stoe & Cie (2002). *X-AREA*. Stoe & Cie, Darmstadt, Germany.
Suckert, S., Rams, M., Böhme, M., Germann, L. S., Dinnebier, R. E., Plass, W., Werner, J. & Näther, C. (2016). *Dalton Trans.* **45**, 18190–18201.
Suckert, S., Rams, M., Germann, L. S., Cegiełka, D. M., Dinnebier, R. E. & Näther, C. (2017). *Cryst. Growth Des.* **17**, 3997–4005.
Böhme, M., Jochim, A., Rams, M., Lohmiller, T., Suckert, S., Schnegg, A., Plass, W. & Näther, C. (2020). *Inorg. Chem.* **59**, 5325–5338.
Brandenburg, K. & Putz, H. (1999). *DIAMOND*. Crystal Impact GbR, Bonn, Germany.
Capacchi, L., Gasparri, G. F., Nardelli, M. & Pelizzi, G. (1968). *Acta Cryst.* B**24**, 1199–1204.

Suckert, S., Wöhlert, S. & Näther, C. (2015). *Inorg. Chim. Acta*, **432**, 96–102.

Wattanakanjana, Y., Nimthong-Roldán, A. & Ratthiwan, J. (2015). *Acta Cryst.* E**71**, m61–m62.

Werner, J., Rams, M., Tomkowicz, Z., Runčevski, T., Dinnebier, R. E., Suckert, S. & Näther, C. (2015b). *Inorg. Chem.* **54**, 2893–2901.

Werner, J., Tomkowicz, Z., Reinert, T. & Näther, C. (2015c). *Eur. J. Inorg. Chem.* pp. 3066–3075.

Werner, S., Tomkowicz, Z., Rams, M., Ebbinghaus, S. G., Neumann, T. & Näther, C. (2015a). *Dalton Trans.* **44**, 14149–14158.

Westrip, S. P. (2010). *J. Appl. Cryst.* **43**, 920–925.

Wöhlert, S. & Näther, C. (2013). *Inorg. Chim. Acta*, **406**, 196–204.

Zhang, S.-G., Li, W.-N. & Shi, J.-M. (2006a). *Acta Cryst.* E**62**, m3398–m3400.

Zhang, S.-G., Li, W.-N. & Shi, J.-M. (2006b). *Acta Cryst.* E**62**, m3506–m3608.

Crystal structure of bis(*N*,*N*′-dimethylthiourea-*κS*)bis(thiocyanato-*κN*)cobalt(II)

Aleksej Jochim, Rastko Radulovic, Inke Jess and Christian Näther

Computing details

Data collection: *X-AREA* (Stoe & Cie, 2002); cell refinement: *X-AREA* (Stoe & Cie, 2002); data reduction: *X-AREA* (Stoe & Cie, 2002); program(s) used to solve structure: *SHELXS97* (Sheldrick, 2008); program(s) used to refine structure: *SHELXL2018/3* (Sheldrick, 2015); molecular graphics: *XP* (Sheldrick, 2008) and *DIAMOND* (Brandenburg & Putz, 1999); software used to prepare material for publication: *publCIF* (Westrip, 2010).

Bis(*N*,*N*′-dimethylthiourea-*κS*)bis(thiocyanato-*κN*)cobalt(II)

Crystal data

$[Co(C_3H_8N_2S)_2(NCS)_2]$	$F(000) = 1576$
$M_r = 383.44$	$D_x = 1.540$ Mg m^{-3}
Monoclinic, $C2/c$	Mo $K\alpha$ radiation, $\lambda = 0.71073$ Å
$a = 16.8070$ (8) Å	Cell parameters from 3218 reflections
$b = 14.4212$ (6) Å	$\theta = 2.0–26.0°$
$c = 15.5669$ (9) Å	$\mu = 1.54$ mm^{-1}
$\beta = 118.744$ (4)°	$T = 200$ K
$V = 3308.1$ (3) Å^3	Block, blue
$Z = 8$	$0.10 \times 0.08 \times 0.07$ mm

Data collection

Stoe IPDS-2 diffractometer	2767 reflections with $I > 2\sigma(I)$
ω scans	$\theta_{max} = 26.0°$, $\theta_{min} = 2.0°$
3218 measured reflections	$h = -20 \rightarrow 19$
3218 independent reflections	$k = -17 \rightarrow 17$
	$l = -2 \rightarrow 19$

Refinement

Refinement on F^2	Hydrogen site location: mixed
Least-squares matrix: full	H-atom parameters constrained
$R[F^2 > 2\sigma(F^2)] = 0.039$	$w = 1/[\sigma^2(F_o^2) + (0.0632P)^2 + 1.3645P]$
$wR(F^2) = 0.105$	where $P = (F_o^2 + 2F_c^2)/3$
$S = 1.07$	$(\Delta/\sigma)_{max} = 0.001$
3218 reflections	$\Delta\rho_{max} = 0.72$ e Å^{-3}
178 parameters	$\Delta\rho_{min} = -0.40$ e Å^{-3}
0 restraints	

Special details

Geometry. All esds (except the esd in the dihedral angle between two l.s. planes) are estimated using the full covariance matrix. The cell esds are taken into account individually in the estimation of esds in distances, angles and torsion angles; correlations between esds in cell parameters are only used when they are defined by crystal symmetry. An approximate (isotropic) treatment of cell esds is used for estimating esds involving l.s. planes.

Refinement. Refined as a 2-component twin.

Fractional atomic coordinates and isotropic or equivalent isotropic displacement parameters (Å²)

	x	*y*	*z*	U_{iso}*/U_{eq}
Co1	0.500000	0.35611 (3)	0.750000	0.04070 (15)
Co2	0.000000	0.64084 (3)	0.250000	0.04322 (15)
N1	0.38555 (14)	0.28706 (15)	0.69242 (15)	0.0454 (5)
C1	0.30981 (16)	0.26507 (16)	0.65171 (17)	0.0399 (5)
S1	0.20412 (4)	0.23531 (6)	0.59318 (5)	0.0602 (2)
N2	0.11433 (14)	0.70960 (15)	0.30776 (16)	0.0488 (5)
C2	0.19017 (16)	0.73153 (16)	0.34319 (17)	0.0414 (5)
S2	0.29563 (4)	0.76089 (6)	0.39174 (6)	0.0609 (2)
S11	0.52044 (4)	0.43897 (5)	0.88607 (5)	0.05212 (19)
C11	0.41958 (16)	0.49900 (16)	0.84464 (17)	0.0404 (5)
N11	0.41916 (14)	0.58993 (14)	0.85125 (16)	0.0464 (5)
H11	0.366818	0.618316	0.831086	0.056*
C12	0.5004 (2)	0.64714 (19)	0.8938 (3)	0.0603 (7)
H12A	0.539073	0.629383	0.962335	0.090*
H12B	0.483201	0.712509	0.890419	0.090*
H12C	0.533658	0.638091	0.857165	0.090*
N12	0.34179 (14)	0.45328 (15)	0.80762 (17)	0.0525 (5)
H12	0.346693	0.392461	0.809838	0.063*
C13	0.25300 (16)	0.4945 (2)	0.7730 (2)	0.0596 (7)
H13A	0.247660	0.518724	0.828810	0.089*
H13B	0.206126	0.447472	0.738940	0.089*
H13C	0.245126	0.545309	0.727713	0.089*
S21	−0.01638 (5)	0.55786 (6)	0.36690 (6)	0.0628 (2)
C21	0.08297 (16)	0.49509 (18)	0.42795 (17)	0.0448 (5)
N21	0.08038 (14)	0.40531 (15)	0.43729 (16)	0.0494 (5)
H21	0.131208	0.377325	0.478147	0.059*
C22	−0.0021 (2)	0.3505 (2)	0.3986 (3)	0.0710 (9)
H22A	−0.037573	0.369132	0.430511	0.107*
H22B	0.013644	0.284667	0.411331	0.107*
H22C	−0.037934	0.360733	0.327816	0.107*
N22	0.16179 (14)	0.53884 (16)	0.46741 (18)	0.0562 (6)
H22	0.158916	0.599750	0.468078	0.067*
C23	0.24956 (16)	0.4953 (2)	0.5241 (2)	0.0584 (7)
H23A	0.254623	0.471054	0.585312	0.088*
H23B	0.297563	0.541035	0.538953	0.088*
H23C	0.255899	0.444206	0.486232	0.088*

Atomic displacement parameters (Å²)

	U^{11}	U^{22}	U^{33}	U^{12}	U^{13}	U^{23}
Co1	0.0279 (2)	0.0390 (3)	0.0494 (3)	0.000	0.0138 (2)	0.000
Co2	0.0258 (2)	0.0420 (3)	0.0532 (3)	0.000	0.0121 (2)	0.000
N1	0.0382 (11)	0.0428 (11)	0.0500 (11)	−0.0038 (9)	0.0171 (9)	0.0013 (9)

C1	0.0369 (12)	0.0355 (11)	0.0441 (11)	−0.0007 (9)	0.0169 (10)	0.0046 (9)
S1	0.0349 (4)	0.0658 (5)	0.0642 (4)	−0.0127 (3)	0.0112 (3)	0.0176 (3)
N2	0.0359 (11)	0.0480 (12)	0.0564 (12)	−0.0041 (9)	0.0173 (9)	−0.0074 (9)
C2	0.0343 (12)	0.0383 (12)	0.0472 (12)	−0.0009 (9)	0.0162 (10)	−0.0027 (10)
S2	0.0338 (4)	0.0657 (5)	0.0756 (5)	−0.0133 (3)	0.0202 (3)	−0.0155 (4)
S11	0.0319 (3)	0.0517 (4)	0.0584 (4)	0.0053 (3)	0.0103 (3)	−0.0126 (3)
C11	0.0342 (12)	0.0430 (13)	0.0427 (11)	−0.0007 (9)	0.0174 (10)	−0.0042 (9)
N11	0.0359 (10)	0.0408 (11)	0.0594 (12)	0.0012 (8)	0.0204 (9)	0.0004 (9)
C12	0.0480 (16)	0.0447 (15)	0.0811 (19)	−0.0081 (12)	0.0252 (14)	0.0004 (13)
N12	0.0337 (11)	0.0430 (11)	0.0722 (14)	−0.0023 (9)	0.0185 (10)	−0.0081 (10)
C13	0.0315 (15)	0.065 (2)	0.0759 (18)	0.0008 (11)	0.0205 (13)	−0.0055 (14)
S21	0.0330 (3)	0.0697 (5)	0.0821 (5)	0.0105 (3)	0.0248 (3)	0.0292 (4)
C21	0.0336 (12)	0.0530 (15)	0.0435 (12)	−0.0003 (10)	0.0152 (10)	0.0039 (10)
N21	0.0381 (11)	0.0438 (12)	0.0560 (12)	−0.0009 (9)	0.0145 (10)	−0.0041 (9)
C22	0.0503 (18)	0.0550 (18)	0.094 (2)	−0.0149 (14)	0.0233 (16)	−0.0172 (16)
N22	0.0337 (11)	0.0455 (12)	0.0771 (15)	0.0016 (9)	0.0169 (11)	0.0117 (11)
C23	0.0309 (15)	0.061 (2)	0.0665 (16)	0.0046 (11)	0.0103 (12)	0.0036 (13)

Geometric parameters (Å, º)

Co1—N1^i	1.959 (2)	C2—S2	1.614 (2)
Co1—N1	1.959 (2)	S11—C11	1.728 (2)
Co1—S11	2.3093 (7)	C11—N11	1.316 (3)
Co1—S11^i	2.3093 (7)	C11—N12	1.323 (3)
Co2—N2^{ii}	1.955 (2)	N11—C12	1.454 (4)
Co2—N2	1.955 (2)	N12—C13	1.448 (3)
Co2—S21	2.3024 (8)	S21—C21	1.728 (3)
Co2—S21^{ii}	2.3024 (8)	C21—N21	1.306 (3)
N1—C1	1.161 (3)	C21—N22	1.322 (3)
C1—S1	1.616 (2)	N21—C22	1.451 (4)
N2—C2	1.163 (3)	N22—C23	1.448 (3)
N1^i—Co1—N1	118.89 (13)	C2—N2—Co2	165.2 (2)
N1^i—Co1—S11	99.39 (6)	N2—C2—S2	179.3 (2)
N1—Co1—S11	111.28 (6)	C11—S11—Co1	103.32 (8)
N1^i—Co1—S11^i	111.28 (6)	N11—C11—N12	119.3 (2)
N1—Co1—S11^i	99.39 (6)	N11—C11—S11	120.75 (18)
S11—Co1—S11^i	117.68 (4)	N12—C11—S11	119.95 (18)
N2^{ii}—Co2—N2	119.05 (13)	C11—N11—C12	124.2 (2)
N2^{ii}—Co2—S21	99.35 (7)	C11—N12—C13	125.6 (2)
N2—Co2—S21	111.39 (7)	C21—S21—Co2	104.82 (8)
N2^{ii}—Co2—S21^{ii}	111.39 (7)	N21—C21—N22	120.1 (2)
N2—Co2—S21^{ii}	99.35 (7)	N21—C21—S21	120.37 (18)
S21—Co2—S21^{ii}	117.37 (5)	N22—C21—S21	119.5 (2)
C1—N1—Co1	165.2 (2)	C21—N21—C22	124.8 (2)
N1—C1—S1	178.9 (2)	C21—N22—C23	125.1 (2)

Symmetry codes: (i) −*x*+1, *y*, −*z*+3/2; (ii) −*x*, *y*, −*z*+1/2.

Hydrogen-bond geometry (Å, º)

D—H···*A*	*D*—H	H···*A*	*D*···*A*	*D*—H···*A*
N11—H11···S1ⁱⁱⁱ	0.88	2.65	3.341 (2)	136
N12—H12···N1	0.88	2.69	3.282 (3)	126
N12—H12···S2^{iv}	0.88	2.88	3.582 (2)	138
C13—H13*B*···S21^v	0.98	2.80	3.578 (3)	137
N21—H21···S1	0.88	2.61	3.372 (2)	146
C22—H22*A*···S2^{vi}	0.98	3.01	3.591 (3)	120
C22—H22*A*···S21^v	0.98	3.02	3.752 (4)	132
N22—H22···S2^{vii}	0.88	2.79	3.486 (3)	137

Symmetry codes: (iii) −*x*+1/2, *y*+1/2, −*z*+3/2; (iv) *x*, −*y*+1, *z*+1/2; (v) −*x*, −*y*+1, −*z*+1; (vi) *x*−1/2, *y*−1/2, *z*; (vii) −*x*+1/2, −*y*+3/2, −*z*+1.